Dynamics of Na^+-Cl^-, Na^+-Na^+, and Cl^--Cl^- Ion Pairs in Dimethyl Sulfoxide: Friction Kernels and Transmission Coefficients

Ashok K. Das,[†] M. Madhusoodanan,[‡] and B. L. Tembe*

Department of Chemistry, Indian Institute of Technology, Bombay Powai, Mumbai, 400 076, India

Received: May 21, 1996; In Final Form: February 5, 1997[⊗]

The dynamics of association of Na^+-Cl^-, Na^+-Na^+, and Cl^--Cl^- ion pairs in liquid dimethyl sulfoxide is studied by using the method of constrained molecular dynamics. Mean force potentials are employed to investigate the role of the solvent on the ion pairs. Friction kernels for the relative dynamics of the ion pairs have been evaluated at several interionic distances. Kramers and Grote−Hynes theories are applied to understand the passage of the ion pairs across the potential energy barrier existing between a contact ion pair and a solvent-separated ion pair. Transmission coefficients for the Na^+-Cl^- ion pair calculated from the above theories are in good agreement with the direct computer simulation results. The magnitudes of the squares of the nonadiabatic barrier frequencies are very large, and these confirm a polarization caging of the reactant ion pairs by the large solvent molecules.

1. Introduction

Association and dissociation of ions in solution media are important in influencing the rates of many chemical reactions.[1−5] The dynamical features associated with the movement of ions in liquid state reactions modify the rate constant obtained by the transition state theory (TST). These may be studied by computing the corresponding transmission coefficients. The influence of the solvent in affecting the forward and the backward rates of a reaction can be studied by calculating reaction flux time correlation functions for both processes.[6−8] Molecular dynamics (MD) simulations[9] offer a straightforward way for calculating these time correlation functions, and thereby the corresponding transmission coefficients.[10−13]

Dimethyl sulfoxide (DMSO) is an organic solvent that finds a wide range of applications in biological reactions.[14] Its utility as a versatile solvent for a vast majority of biochemical reactions stimulates one to acquire the knowledge of its ability to solvate ions, ion pairs, and other molecular species, the dynamics of these species in DMSO, and finally the reaction flux time correlation functions between reacting species. For the present study, we have selected the sodium chloride ion pair for its well-known applicability in chemistry and biochemistry.[15] The first molecular dynamics simulations on DMSO were reported by Rao and Singh.[16] These authors determined the relative difference in the free energies of solvation between different ions in DMSO. MD simulations on water−DMSO mixtures have also been reported.[17] The structure and dynamics of hydrogen bonding in water−DMSO mixtures have been extensively studied through MD simulations.[18]

In the recent past, the equilibrium aspects of the ion pair interconversion process have been the subject of both theoretical[19−23] and computer simulation[13,24−30] studies. Several ionic species in different polar solvents have been investigated. Usually these studies dwell on the calculation of the potentials of mean force (pmf), $W(r)$, and the friction kernels, $\xi(t)$, due to the solvent molecules around the reactant ions, vis à vis direct computation of the dynamical transmission coefficient, $\kappa(t)$, through MD simulations.[13,29] The pmf between an ion pair at a given interionic separation is the work done to bring the two ions up to that separation in the presence of the solvent medium. The pmf can be obtained by constrained molecular dynamics simulations performed over a representative set of interionic separations in the presence of a sufficient number of solvent molecules around the ions. In terms of the solute−solute (i.e. ion−ion) radial distribution function $g(r)$, the pmf $W(r)$ is given by[31]

$$W(r) = -k_B T \ln[g(r)] \tag{1}$$

where r is the interionic distance, k_B, the Boltzmann constant, and T, the temperature. The friction kernel, $\xi(t)$, for the relative dynamics of ion pairs in a solvent is defined as[32,33]

$$\xi(t) = (\mu k_B T)^{-1} \langle R(t) \cdot R(0) \rangle \tag{2}$$

where μ is the reduced mass of the ion pair, $R(t)$ is the stochastic force along the interionic axis at time t, and $\langle \ldots \rangle$ denotes the ensemble average.

The use of the pmfs for the ionic dissociation−association of sodium chloride in solvents such as water,[11,34] methanol,[35] and dimethyl sulfoxide[36] has demonstrated the role of the solvent in determining the location of the first local minimum in the pmfs [e.g., 2.9 Å in water, 2.6 Å in methanol, and 2.6 Å in DMSO; the gas phase minimum in the potential is at 2.5 Å] and in contributing to different barriers for ionic dissociation−association. The calculation of the friction kernels for water[33] and methanol[35] has been performed by Guardia et al. In the present paper, we report the calculation of the friction kernels in DMSO and investigate the influence of solvent $\xi(t)$ on the reaction rate constants. The dynamical aspects of the ion pair interconversion process can also be probed through direct MD simulations as detailed by several authors.[11,13,28] We have also computed the dynamic transmission coefficient for the Na^+-Cl^- ion pair in DMSO through these direct MD simulations. The results are then compared with the predictions of Kramers[37] and Grote−Hynes[38] theories.

The organization of this article is as follows. In section 2, we present a brief description of the models used and the methods employed in the MD simulations. The structure and dynamics of the ion pairs are described in section 3. Analysis

[†] On leave from the Department of Technical and Applied Chemistry, Victoria Jubilee Technical Institute, Matunga, Mumbai, 400 019, India.

[‡] Present address: Department of Chemistry, Bar Ilan University, Ramat-Gan 52900, Israel.

[⊗] Abstract published in *Advance ACS Abstracts,* March 15, 1997.

S1089-5639(96)01455-7 CCC: $14.00

TABLE 1: Site−Site Potential Parameters for DMSO, Na^+ Ion, and Cl^- Ion

site	$10^{-4}\ A_{\alpha\beta}$, k_BT Å^{12}	$10^{-2}\ C_{\alpha\beta}$, k_BT Å^6
S	565.0	27.7
CH_3	511.8	23.5
O	18.6	2.9
Na^+	2.4	5.1
Cl^-	4390.5	59.1

of the results in terms of Kramers and Grote−Hynes theories is presented in section 4. In section 5, we have investigated the ion pair interconversion process through direct MD simulations. The conclusions of the present work are summarized in the last section.

2. The Model and the Method

The details of the molecular model of DMSO and the charge distribution around the atomic sites have been described by us in our earlier paper.[36] While the same reference should be consulted for details, we recount here the important features relevant to the present work. We have used the charge distribution obtained by Rao and Singh,[16] namely, S (+0.139*e*), O (−0.459*e*), and CH_3 (+0.160*e*), where *e* is the magnitude of electronic charge. The intermolecular associations in DMSO and its aqueous solutions are due to the polarization of the sulfur−oxygen bond,[14] for which the bond order is 1.55. We have made use of the neutron diffraction data on liquid DMSO, reported by Bertagnolli et al.,[38] for our calculations. The bond lengths are S−O (1.496 Å) and S−C (1.8 Å); the bond angles are O−S−C (107.2°) and C−S−C (99.2°).

The intermolecular potentials are defined as follows. The solvent−solvent, solute−solvent, and solute−solute potentials are taken as the sum of the Lennard-Jones (LJ) and Coulombic terms.[13,30] The site−site potential has been taken as

$$U_{\alpha\beta}(r) = (A_{\alpha\beta}/r^{12}) - (C_{\alpha\beta}/r^6) + (q_\alpha q_\beta/r) \qquad (3)$$

where α and β are the interaction sites on different molecules, *r* is the site−site separation, and q_α and q_β are the charges located at the sites α and β, respectively. Table 1 lists the values of the site−site potential parameters, $A_{\alpha\beta}$ and $C_{\alpha\beta}$, in units of k_BT.

The system we have considered for the MD simulations contains 125 DMSO molecules and one of the three ion pairs. The length of the cubic simulation box was taken to be 24.506 Å. An average temperature of 298 K was maintained. This gurantees an approximate density of 1.1 g/cm^3 for DMSO at the simulation temperature. Conventional periodic boundary conditions were imposed to simulate the microcannonical ensemble. Earlier MD simulations done on DMSO by Vaisman and Berkowitz[17] taking 64 and 512 molecules resulted in a fairly similar structure of the site−site radial distribution functions. These authors used the same interaction potentials as defined by eq 3. For our purpose, we have compared the simulation results in (a) 125 DMSO molecules in a cubic simulation cell of edge length 24.506 Å and (b) 254 DMSO molecules in a cubic simulation cell of edge length 31.039 Å, both yielding the same values (within 1%) for the solvent friction coefficient. To truncate the short-range (ion−DMSO) and (DMSO−DMSO) interactions, a spherical cutoff with half the box length as the cutoff radius was used. The long-range interactions were computed using the reaction field technique.[40,41] The equations of motion for the solvent particles were solved numerically using the Verlet algorithm.[42] We have used 0.005 ps as the time step in the MD simulations. To maintain the intramolecular structure of DMSO and also to hold the interionic distance constant, the SHAKE algorithm[43] was used. For each of the interionic separations, the system was equilibrated for 50 ps.

For the system consisting of two ions (A,B) and *N* solvent molecules, the force due to the solute−solvent interactions acting along the interionic axis can be evaluated as[33,35,44]

$$\Delta F(t;r) = \mu\left\{\frac{F_{AS}(t;r)}{m_A} - \frac{F_{BS}(t;r)}{m_B}\right\}\cdot\hat{r} \qquad (4)$$

where $F_{AS}(t;r)$ and $F_{BS}(t;r)$ are the total forces on the solute particles due to the solvent molecules; m_A and m_B are the individual masses of the ions; μ is the reduced mass; and $\hat{r}$ is the unit vector along the AB direction. The $F(t;r)$ values were calculated at each time step and then averaged over the whole simulation. The total mean force between the ions is the sum of the direct ion−ion force, $F_d(r)$, and the solvent contribution, $\Delta F(r)$. That is,

$$F(r) = F_d(r) + \Delta F(r) \qquad (5)$$

where $\Delta F(r) \equiv \langle \Delta F(t;r)\rangle$. The potential of mean force can then be calculated as[28,30,35]

$$W(r) = -\int F(r)\,\mathrm{d}r = W(r_0) - \int_{r_0}^{r} F(r)\,\mathrm{d}r \qquad (6)$$

The choice of $W(r_0)$ was done in such a way that the calculated mean force potentials match the macroscopic Coulombic potential at long distances.[45] We have found that the pmf is not sensitive to the choice of r_0 at a distance greater than 7.8 Å.

To provide for a tool for the analysis of the relative dynamics of the ion pairs, we have calculated the friction kernels, $\xi(t)$, using eq 2. The stochastic forces responsible for the solvent friction can simply be obtained as[29,33]

$$R(t) = \Delta F(t;r) - \Delta F(r) \qquad (7)$$

under the rigid bond approximation for the solute ion pair. As a prerequisite for eq 7, the systems considered must have clear separation of time scales for the translational and reorientational motion of the ion pair. This condition has been verified for the Na^+−Cl^- ion pair by Guardia et al.[29] for associated liquids (such as water) and is expected to be valid for heavier and moderately associating liquids. Thus, one can use eqs 2 and 7 to evaluate the friction kernels in the constrained MD simulations.

3. Structure and Dynamics of the Na^+−Cl^- Ion Pair

The main characteristics of the potentials of mean force for the three ion pairs in different solvents are given in Table 2 for comparison. The potentials of mean force for the Na^+−Cl^- ion pair in DMSO were calculated and reported by Madhusoodanan and Tembe.[36] Figure 1 presents the essential features of the pmfs of the Na^+−Cl^-, Na^+−Na^+, and Cl^-−Cl^- ion pairs in DMSO. The $W(r)$ of the Na^+−Cl^- pair shows two minima: a deep minimum at $r = 2.6$ Å and a shallow minimum at $r = 7.2$ Å. At interionic separation of $r = 4.9$ Å the pmf has a local maximum of ca. 1.7 k_BT. The first minimum at 2.6 Å corresponds to the contact ion pair (CIP), where the Na^+ and Cl^- ions are held in close contact by the strong electrostatic attractive forces. The second shallow minumum at 7.2 Å represents the solvent-separated ion pair (SSIP), where the two ions are held together with one solvent molecule between them. Figure 2 presents the representative configurations of the solvent molecules (within 5 Å from either ion) around the three ion pairs at selected interionic distances.

TABLE 2: Main Characteristics of the pmf's of Na^+-Cl^-, Na^+-Na^+ and Cl^--Cl^- Ion Pairs in Different Solvents

	in water[a]		in methanol[b]		in DMSO[c]	
ionic species	r/ Å	$W(r)$/ (k_BT)	r/ Å	$W(r)$/ (k_BT)	r/ Å	$W(r)$/ (k_BT)
(Na^+-Cl^-)						
first minimum	2.9	−1.04	2.6	−5.83	2.6	−27.03
first maximum	3.7	+1.46	3.4	−0.42	4.9	+1.69
second minimum	5.0	−2.08	4.6	−5.21	7.2	−0.25
(Na^+-Na^+)						
first minimum	3.8	+0.21	3.6	+9.00	3.6	+10.14
first maximum	5.0	+1.67	4.6	+10.40	4.9	+13.52
	6.0	+0.42	6.0	+6.80	7.0	+5.07
(Cl^--Cl^-)						
	5.4	+1.33	5.4	+13.33	5.4	+11.83
	6.4	+2.00	7.8	+2.67	7.8	+1.54

[a] Reference 33. [b] Reference 35. [c] Reference 30.

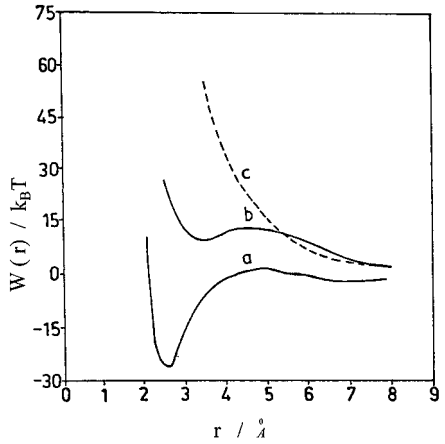

Figure 1. Potentials of mean force for the (a) Na^+-Cl^- (b) Na^+-Na^+, and (c) Cl^--Cl^- ion pairs in dimethyl sulfoxide.

Because of the shallow barrier ($\sim$1.7 k_BT) in the pmf of Na^+-Cl^- to move from a SSIP configuration to a CIP configuration, we expect that many of the SSIPs would have a rather large probability of crossing the SSIP → CIP barrier to assume a CIP configuration. The activated process would thus be expected to possess a first-order rate constant. The other factors influencing the kinetics of the process are the solvent reorientational motions as well as the influence of other CIP/SSIPs present in the system. The deep potential minimum at 2.6 Å for the CIP indicates a very stable configuration for the contact ion pair. The longer distance of the ion pair in the SSIP configuration in DMSO is because of the large size of the solvent molecules.

By comparison, the Na^+-Cl^- ion pair shows an association barrier of 3.7 k_BT in water,[29] 5.6 k_BT in methanol,[35] and 1.9 k_BT in DMSO. Thus, the ion association in DMSO is a highly favored process.

Under the rigid bond approximation (for the ion pair), the initial time values of the $\xi(t)$ kernels are dependent not only on the interionic separations but also on the nature of the solvents. Table 3 presents a comparison of the initial values of the friction kernels at several interionic distances for the Na^+-Cl^-, Na^+-Na^+, and Cl^--Cl^- ion pairs. The interionic distances in each of the Na^+-Cl^- and Na^+-Na^+ are chosen as the first minimum, first maximum, and second minimum, respectively. The pmf of the Cl^--Cl^- ion pair does not have any minimum in any of the solvents; consequently, the interionic distances (referred to in Table 3) were chosen to broadly cover the 4.0−8.0 Å region. The results obtained for water[33] and methanol[35] show an increase in the initial values of the friction kernels with increasing interionic separations. Such a generalization is not observed in the case of the Na^+-Cl^- ion pair in DMSO. This may be attributed to the already large interionic distance of the ion pair in the transition state (4.9 Å) and also to the need for the ions to separate further before an individual ion is fully surrounded by its own solvation shell.

The normalized friction kernels [$\xi_N(t) = \xi(t)/\xi(0)$] associated with the Na^+-Cl^-, Na^+-Na^+, and Cl^--Cl^- ion pairs in DMSO at several interionic distances are displayed in Figures 3, 4, and 5, respectively. We now compare the overall shapes of the normalized friction kernels for each of the ion pairs in water, in methanol, and in DMSO. All the $\xi_N(t)$'s show very rapid initial decays for the Na^+-Cl^- ion pair, and these decays are nearly identical up to a time of about 0.1 ps. This rapid decay is followed by a long-time decay characteristic of each system. The initial negative oscillations in the decay of the $\xi_N(t)$'s of the Na^+-Cl^- ion pair are more pronounced in DMSO than in methanol and in water. In DMSO, the oscillations persist up to 0.5 ps, while in methanol they persist up to 0.2 ps and in water the oscillations persist only up to 0.1 ps. To confirm these oscillations, we have estimated the errors in $\xi_N(t)$ from 10 MD runs, each of 40 ps. The errors in $\xi_N(t)$ are <5% in the range 0−0.1 ps and <10% in the range 0.1−0.5 ps. Beyond 0.5 ps, $\xi_N(t)$ has already decayed to less than 0.05 in magnitude. Thus, the negative oscillations in the 0−0.5 ps range are statistically significant.

The differences of the $\xi_N(t)$ values at the three interionic distances are smaller in DMSO and in water than in methanol. As a matter of fact, the $\xi_N(t)$ value in methanol[35] at the shortest interionic distance of 2.6 Å does not decay to zero even at 1.25 ps and remains above 0.2 over the entire period from 0.0 to 1.25 ps. The difference between $\xi_N(t)$ at 2.6 Å and $\xi_N(t)$ at 3.4 Å in methanol is about 0.3 over the period 0.0−1.25 ps; likewise, the difference in $\xi_N(t)$ values between 2.6 and 4.6 Å is close to 0.2 over the same time period. In the case of DMSO, a smaller difference of 0.1 in $\xi_N(t)$ values exists only between 0.05 and 0.5 ps for the shorter (2.6 Å) and the longer (4.9 and 7.2 Å) interionic distances. Several factors such as molecular shape, molecular mass, and symmetry could contribute to this. It would be interesting to study the specific effects of polarity on these differences. The friction kernels in water are the least structured at the interionic distances reported.[33]

The observed behavior of $\xi_N(t)$'s of the Na^+-Na^+ ion pair is very similar in all three solvents. Short-time negative oscillations in $\xi_N(t)$ are observed in water (up to 0.1 ps), in methanol (up to 0.2 ps), and in DMSO (up to 0.6 ps). The short distance ($r_{Na-Na} \approx 3.6$ Å) $\xi_N(t)$ is distinctly different from the large-distance ($r_{Na-Na} \geq 4.5$ Å) $\xi_N(t)$. In methanol, the differences in $\xi_N(t)$ values at the three interionic distances persist over the entire period from 0.0 to 1.25 ps and the long-time $\xi_N(t)$ for the $r_{Na-Na} = 3.6$ Å decays only up to 0.1 at 1.25 ps. In water and in DMSO, the differences between short-distance $\xi_N(t)$ and large-distance $\xi_N(t)$ persist only between 0.05 and 0.5 ps. Strong structural similarities in the solvent organization around the two Na^+ ions are responsible for influencing the dynamics of the solvent molecules for these ions over the range of interionic distances considered. The friction kernels for the Cl^--Cl^- ion pair exhibit the slowest decay. The dependence of $\xi_N(t)$ for this ion pair on the interionic separation is negligible in all three solvents. The characteristic oscillatory behavior of $\xi_N(t)$ is also the least for this ion pair.

It may be noted that for the Na^+-Cl^- ion pair in DMSO the $\xi_N(t)$ at an interionic distance corresponding to the minimum of $W(r)$ at 2.6 Å has a distinct short-time (up to 0.25 ps) decay pattern in the sense that the negative oscillations are the least pronounced. Similar behavior of $\xi_N(t)$ of the same ion pair was

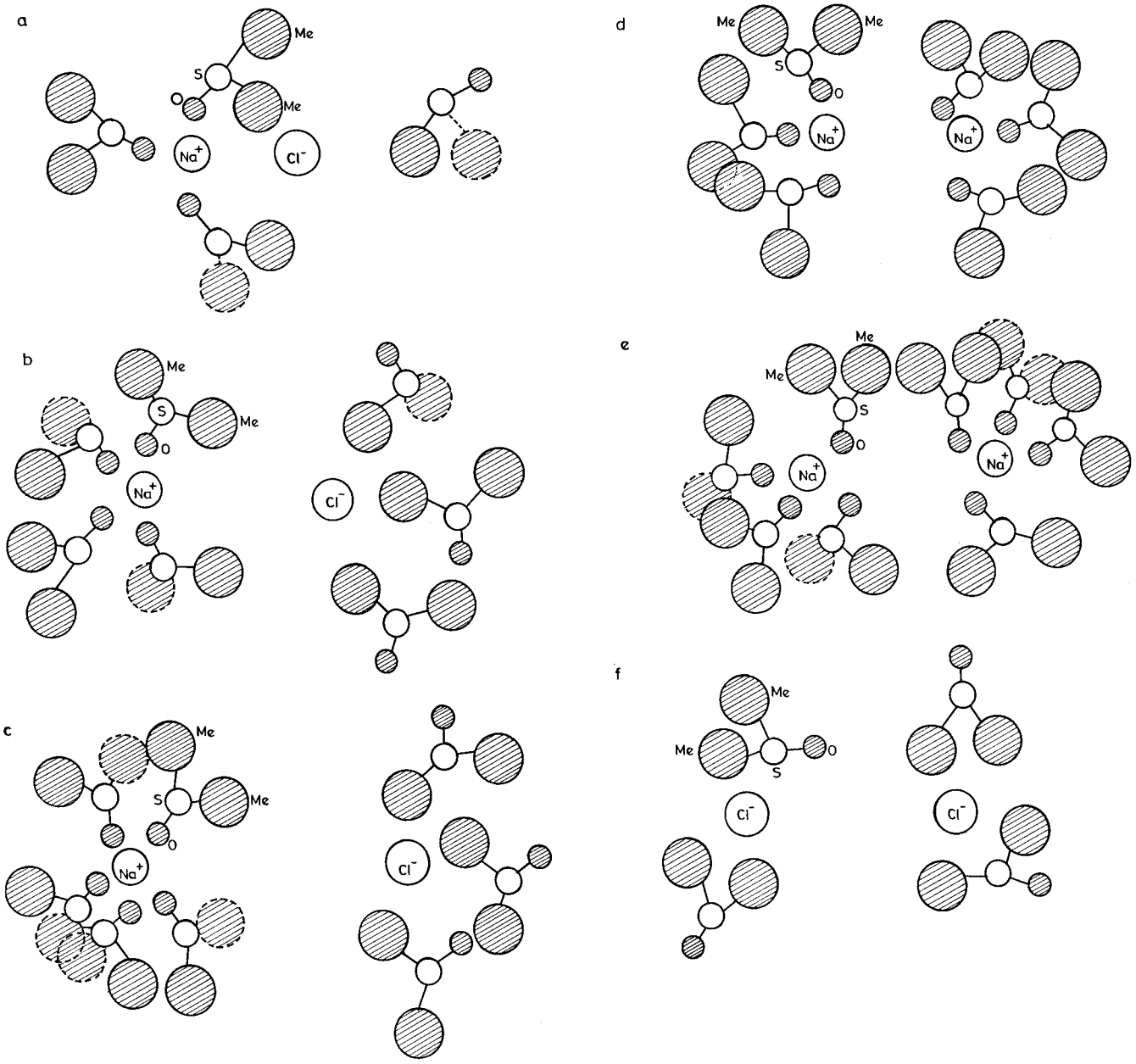

Figure 2. Characteristic solvent configurations around the reactant ion pairs in DMSO: (a) Na^+-Cl^- at 2.6 Å; (b) Na^+-Cl^- at 4.9 Å; (c) Na^+-Cl^- at 7.2 Å; (d) Na^+-Na^+ at 3.6 Å; (e) Na^+-Na^+ at 4.9 Å; (f) Cl^--Cl^- at 5.4 Å. (See text.)

TABLE 3: Initial Values of the Friction Kernels of Na^+-Cl^-, Na^+-Na^+, and Cl^--Cl^- Ion Pairs at Several Interionic Distances

	in water[a]		in methanol[b]		in DMSO[c]	
ionic species	r (Å)	$\xi(0) \times 10^{-3}$ (ps^{-2})	r (Å)	$\xi(0) \times 10^{-3}$ (ps^{-2})	r (Å)	$\xi(0) \times 10^{-3}$ (ps^{-2})
Na^+-Cl^-	3.0	1.38	2.6	1.32	2.6	7.7 ± 0.2
	3.7	2.00	3.4	1.47	4.9	10.7 ± 0.6
	5.0	2.36	4.6	1.78	7.2	10.6 ± 0.8
Na^+-Na^+	3.8	2.45	3.6	2.20	3.6	7.3 ± 0.4
	5.0	2.87	4.6	2.31	4.9	8.4 ± 0.3
	6.0	2.79	6.0	2.56	7.0	8.6 ± 0.2
Cl^--Cl^-	5.4	1.34	5.4	0.70	5.4	1.1 ± 0.1
	6.4	1.37			7.8	1.0 ± 0.1

[a] Reference 33. [b] Reference 35. [c] Present work.

observed in water[33] and in methanol.[35] These observations also hold good for the Na^+-Na^+ ion pair in all three solvents. The stability and the long-lived character of the CIP configuration are inducing a slower decay of fluctuation in $R(t)$.

4. Ion Pair Interconversion in the Na^+-Cl^- System

To calculate the reaction rates for the transitions between the contact ion pair and the solvent-separated ion pair states, we have evaluated the friction kernels that characterize the dynamics of the process. The rate constant (k_{rate}) of the interconversion (i.e. CIP to SSIP and vice versa) process is related to the corresponding transition state theory value (k_{TST}) by the transmission coefficient (κ)

$$k_{rate} = k_{TST}\kappa \tag{8}$$

The pmfs of the Na^+-Cl^- and the Na^+-Na^+ ion pairs have activation barriers for CIP → SSIP process at the same interionic separation of 4.9 Å. We have determined the corresponding transmission coefficients of these barriers using the Kramers theory[37] and the Grote−Hynes (GH) theory[38] for the ion dissociation−association reactions in solution. Both these theories assume a stochastic equation (here, a generalized Langevin equation)[5,37,46] for the time evolution of the reaction

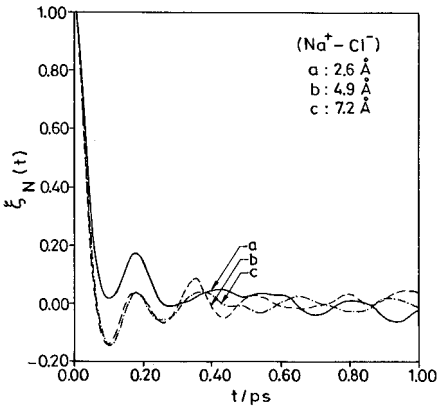

Figure 3. Normalized friction kernels for the Na^+-Cl^- ion pair at several interionic distances.

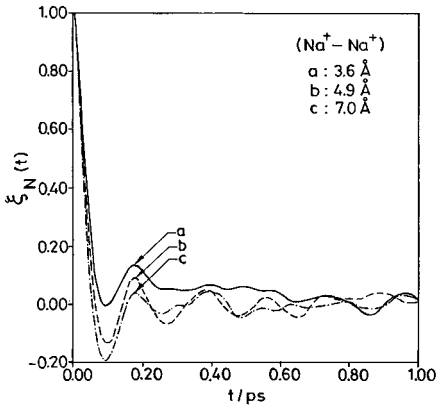

Figure 4. Normalized friction kernels for the Na^+-Na^+ ion pair at several interionic distances.

coordinate (here, the interionic axis). In the Kramers theory, an instantaneous solvent response is implicit for the reactive process. According to Kramers, the transmission coefficient is expressed as[33]

$$\kappa_{Kr} = [1 + (\xi/2\omega_b)^2]^{1/2} - (\xi/2\omega_b) \tag{9}$$

where ξ is the constant friction coefficient[13] given by

$$\xi = \int_0^\infty dt\, \xi(t) \tag{10}$$

and $\xi(t)$ is the time dependent friction coefficient defined by eq 2; ω_b is the barrier frequency[38,47] (obtained in our studies by fitting an inverted parabola[13,46] in the barrier region; i.e., at $r = r^\ddagger \pm 0.5$ Å; where r is the interionic separation and $r^\ddagger$ is the interionic separation at the transition state). The transmission coefficient in the GH theory can be expressed as[38]

$$\kappa_{GH} = \lambda_r/\omega_b \tag{11}$$

where the reactive frequency,[38] λ_r, is the solution of the implicit equation

$$\lambda_r = \omega_b^2/[\lambda_r + \int_0^\infty dt \exp(-\lambda_r t)\, \xi(t)] \tag{12}$$

According to eqs 8 and 11, the rate constant is just the TST rate constant (k_{TST}) times the ratio of the reactive frequency (λ_r) and the barrier frequency (ω_b). Equation 12 demands that we need to know the behavior of $\xi(t)$ at all times during the reactive process. The reciprocal of the reactive frequency (λ_r^{-1}) gives a measure of the time scale characteristic for the reaction coordinate motion at the transition state in the presence of the solvent. When barrier recrossings are neglected, then $\lambda_r = \omega_b$, and the TST applies. The GH approach has been found to give satisfactory results when compared with the MD calculations on ion pair dynamics in model solvents,[13] in water,[33] and in methanol.[35] The dynamic solvent influence that enters into the GH expression (eqs 11 and 12) via the time dependent friction $\xi(t)$ has been successfully utilized in explaining the deviations from the TST for many chemical reactions. These include dipole isomerization,[48] heavy particle charge transfer,[46,49] electron transfer,[50] proton transfer,[51] photochemical charge transfer,[52] and S_N2 reactions.[53]

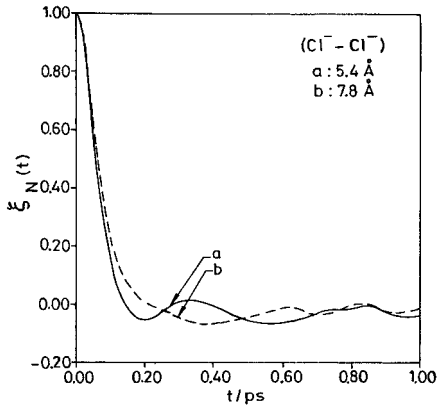

Figure 5. Normalized friction kernels for the Cl^-Cl^- ion pair at several interionic distances.

The various dynamical coefficients involved in the Kramers and the Grote−Hynes expressions for the barrier crossing reactions for the two ion pairs Na^+-Cl^- and Na^+-Na^+ in DMSO are listed in Tables 4 and 5, respectively. For the purpose of comparison, the values obtained for water[33] and methanol[35] are also included in these tables.

As can be seen from Table 4, the barrier frequencies for the Na^+-Cl^- ion pair in the three solvents follow the trend ω_b(methanol) > ω_b(water) > ω_b(DMSO). The barrier in the pmf of the Na^+-Cl^- ion pair in methanol[35] is sharper than in water,[29] which in turn is sharper than in DMSO.[36] We have observed that the barrier in the pmf of water fits an inverted parabola quite well with the error in $\omega_b < 0.2$ ps^{-1}. In the case of methanol and DMSO we have estimated the errors in ω_b by fitting inverted parabolas in three ranges of ±0.4 Å, ± 0.5 Å, and ± 0.6 Å around the barrier top. In methanol the error in ω_b is ±1.0 ps^{-1}, while in DMSO the error is ±1.4 ps^{-1}. For each of the barrier tops, the parabolas match the pmfs within 10%. The magnitudes of the barrier frequencies in these solvents are manifestations of the steepness of the respective pmfs. We observe that the reaction time scale value (λ_r^{-1}) is shortest in methanol (0.10 ps) and longest in DMSO (1.56 ps); the corresponding value in water is 0.28 ps. As λ_r^{-1} gives a measure of the time spent by the reactant ion pair in the transition state, it can be seen that on a rather flat barrier top (like that in DMSO) the transition state configuration is long-lived. The large value of this reaction time scale in DMSO is due to the strong negative oscillations in $\xi_N(t)$ (which make the integral in eq 12 small) and also due to the small value of ω_b.

One can define a "kernel correlation time" (τ_{kc}) characteristic of the solvent through the integral value of the normalized friction kernel,

$$\tau_{kc} = \int_0^\infty dt\, \xi_N(t) \tag{13}$$

This has been referred to as the "solvent time scale" (τ_c) by Rey et al.[33] (for water) and by Sese et al.[35] (for methanol). In these two solvents, the $\xi_N(t)$ for the Na^+-Cl^- ion pair exihibits

TABLE 4: Na^+-Cl^- Association and Dissociation Reactions in Water, in Methanol, and in DMSO

property	in water[a]	in methanol[b]	in DMSO[c]
top barrier position, r (Å)	3.7	3.4	4.9
barrier frequency, ω_b (ps^{-1})	16.1	19.7	11.9
initial friction coefficient, $\xi(0)$ (ps^{-2})	2.00×10^3	1.47×10^3	10.74×10^3
constant friction coefficient, ξ (ps^{-1})	199	80	251
Kramers transmission coefficient, κ_{Kr}	0.08	0.23	0.05
Grote−Hynes transmission coefficient, κ_{GH}	0.22	0.49	0.05
reaction time scale, λ_r^{-1} (ps)	0.28	0.10	1.56
kernel correlation time, τ_{kc} (ps)	0.10	0.054	0.025
kernel decay time, $t_{0.05}$ (ps)	0.79	0.59	0.38
nonadiabatic frequency, ω_{NA}^2 (ps^{-2})	-1.7×10^3	-1.08×10^3	-9.9×10^3

[a] Reference 33. [b] Reference 35. [c] Present work.

TABLE 5: Na^+-Na^+ Association and Dissociation Reactions in Water, in Methanol, and in DMSO

property	in water[a]	in methanol	in DMSO[d]
top barrier position, r (Å)	5.0	4.6[b]	4.9
barrier frequency, ω_b (ps^{-1})	7.9	14.5[c]	15.6
initial friction coefficient, $\xi(0)$ (ps^{-2})	2.87×10^3	2.31×10^3 [b]	8.36×10^3
constant friction coefficient, ξ(ps^{-1})	369	194[c]	166
Kramers transmission coefficient, κ_{Kr}	0.03	0.07[c]	0.09
Grote−Hynes transmission coefficient, κ_{GH}	0.02	0.12[c]	0.08
reaction time scale, λ_r^{-1} (ps)	4.50	0.56[c]	0.83
kernel correlation time, τ_{kc} (ps)	0.13	0.08[c]	0.02
kernel decay time, $t_{0.05}$ (ps)	0.78	0.44[c]	0.40
nonadiabatic frequency, ω_{NA}^2 (ps^{-2})	-2.8×10^3	-2.1×10^3 [c]	-7.9×10^3

[a] Reference 33. [b] Reference 35. [c] Computed from the data given in ref 35. [d] Present work.

a negative oscillation for short periods (up to 0.1 ps in water and up to 0.2 ps in methanol). However, the $\xi_N(t)$ for the same ion pair in DMSO shows a more pronounced negative oscillation for a longer period (up to 0.6 ps). The long-lived oscillatory behavior of the friction kernel in DMSO is a characteristic of this solvent.

Because of the negative oscillations of the friction kernels at short times, the very small magnitudes of τ_{kc} may not yield a suitable comparison of the different solvents. As an alternative measure of the solvent time scale, one can compare the characteristic times of decay of the friction kernel to a low value (say 5% of the initial magnitude) analogous to the half-life $t_{1/2}$ used in chemical kinetics. For the Na^+-Cl^- ion pair, the values for $t_{0.05}$ are 0.79 ps (water), 0.59 ps (methanol), and 0.38 ps (DMSO). Thus, the trends observed in τ_{kc} values are identical with the trends in $t_{0.05}$ values.

It can be seen that τ_{kc} for the Na^+-Cl^- ion pair is shortest in DMSO (0.025 ps) and longest in water (0.10 ps); the corresponding value in methanol is 0.054 ps. This is attributed to the differences in the behavior of the solvent molecules during the reaction. In water, which has a strongly hydrogen-bonded structure, the solvent molecules trap the reactants and move with them during the reactive process.[35] This is also true in methanol, but barrier crossing reactions in methanol may not involve major changes in the linear structures of the hydrogen-bonded chains formed by the solvent molecules.[35] This makes the kernel correlation time τ_{kc} shorter in methanol compared to that in water. In DMSO, the extent of hydrogen bonding is not very significant because of the relatively less polar nature of the two methyl groups (charges $+0.160e$ each) [in water, charges on atoms are H ($+0.410e$), O ($-0.820e$); and in methanol, charges are H ($+0.400e$), O ($-0.685e$), CH_3 ($+0.285e$)], although the molecule has a stronger dipole moment (the dipole moments of water, methanol, and DMSO are 1.82, 2.87, and 4.06 D, respectively[16]). During the barrier crossing reactions in DMSO, the solvent molecules form a tightly bound coordination shell around the positive ion [as evidenced by the (Na^+-O) radial distribution function,[30] peaked at 2.1 Å], but the coordination shell around the negative ion is loosely bound [the (Cl^--CH_3) radial distribution function[30] peaked at 3.8 Å]. Because of this, the solvent cage undergoes very little change during the passage across the activation barrier. Hence τ_{kc} is shortest in DMSO.

The initial value of the friction kernel, $\xi(0)$, is the measure of the magnitude of the fluctuations in the random forces at a given temperature in the solvent medium. Numerically, $\xi(0)$ equals the square of the electrostatic solvent frequency.[46] This also contributes to the resultant behavior of the reacting system to be either in the nonadiabatic regime or in the polarization caging regime.[46,54,55] When in the nonadiabatic regime, the solvent molecules cannot move significantly during the reaction time (λ_r^{-1}); that is, the solvent is effectively frozen during the passage across the barrier top. For this limit, $\omega_{NA}^2 > 0$; where ω_{NA}^2 is the square of the nonadiabatic barrier frequency.[54]

$$\omega_{NA}^2 = \omega_b^2 - \xi(0) \tag{14}$$

The polarization caging regime is characterized by strong solvent forces[46] where $\xi(0)$ exceeds the square of the barrier frequency; i.e. $\xi(0) > \omega_b^2$. In this regime, the motion of the solvent molecules is required for the reaction to occur. The explicit nature of the response of the solvent can be considered as follows. When the ratio $\xi(0)/\omega_b^2$ just exceeds unity, the solvent responds rapidly to the motion of the solute ion pair, but for $\xi(0)/\omega_b^2 \gg 1$, the solvent polarization lags the motion of the solute,[46] retarding the rate much below the k_{TST}. Thus, when the reactant ion pair moves away from the barrier top, it finds itself in an effective potential well of frequency ω_{eff} (with $\omega_{eff}^2 = \xi(0) - \omega_b^2 > 0$). The solvent does not get any time to readjust and the ion pair moves with this solvent shell around it intact. Motion within this polarization cage is oscillatory, and the barrier crossings and recrossings persist for an extended length of time.[46]

We find, for the Na^+-Cl^- ion pair, $\xi(0)$(methanol) < $\xi(0)$(water) $\ll$ $\xi(0)$(DMSO). The initial friction $\xi(0)$ gauges the coupling between the solvent dipoles and the reactant ion pair.[48] Although water molecule is the smallest of the three, its $\xi(0)$ value is more than that in methanol because of its strong hydrogen-bonded character. The negative values of the square

of the nonadiabatic barrier frequencies ω_{NA}^2 for all three solvents indicate strong polarization caging[46] of the reactant Na^+-Cl^- ion pair by the solvent molecules. Finally, the Kramers (κ_{Kr}) and the Grote−Hynes (κ_{GH}) transmission coefficients follow the trend as dictated by the magnitudes of the barrier frequencies in respective solvents. Thus, κ_{Kr}(methanol) > κ_{Kr}(water) > κ_{Kr}(DMSO) and κ_{GH}(methanol) > κ_{GH}(water) > κ_{GH}(DMSO).

From the data presented in Table 5, the barrier frequencies for the Na^+-Na^+ ion pair in the three solvents follow the trend ω_b(DMSO) ≅ ω_b(methanol) > ω_b(water). These ω_b's have been determined by fitting inverted parabolas to the respective pmf's in the range $r = r^{\ddagger} \pm 0.5$ Å. Like before, the magnitudes of ω_b reflect the steepness in the barrier in the pmf's in the presence of the respective solvents. The pmf's of the Na^+-Na^+ ion pair in methanol[35] and in DMSO[30] are equally steep in the barrier regions, although the barrier top positions are different in the two (top barrier position in methanol is at 4.6 Å and that in DMSO is at 4.9 Å). The pmf of the Na^+-Na^+ ion pair in water[34] shows a flat maximum of ca. 1.5 k_BT at 5.0 Å. The small magnitude of ω_b and the short-time negative oscillations in $\xi_N(t)$ for this ion pair make the reaction time scale value (λ_r^{-1}) longest in water (4.50 ps). In DMSO and in methanol, the values of λ_r^{-1} are 0.83 and 0.56 ps, respectively, for nearly equal values of barrier frequencies ($\omega_b = 14.5 \pm 1.5$ ps^{-1} in methanol, and 15.6 ± 1.5 ps^{-1} in DMSO). These results also indicate that small values of ω_b lead to large values of λ_r^{-1} (exemplified by the case of water). For similar values of ω_b, greater negative oscillations in $\xi_N(t)$ tend to give larger values of λ_r^{-1}. This is exemplified here by DMSO and methanol. From the above values of the reaction time scales, we see that the reactant ion pair Na^+-Na^+ in water solvent spends the longest time in the transition state.

The integral value of $\xi_N(t)$ gives the kernel correlation time, τ_{kc} (eq 13) for the reactant ion pair (referred to as the solvent time scale, τ_c, in refs 33 and 35). We find that the τ_{kc} for the Na^+-Na^+ ion pair is shortest in DMSO (0.02 ps), 0.08 ps in methanol, and longest in water (0.13 ps). The times taken by the $\xi_N(t)$ to decay to a small value (say 5% of the initial value) are 0.40 ps (DMSO), 0.44 ps (methanol), and 0.78 ps (water). Thus, the trends in the τ_{kc} values are identical to the trends in $t_{0.05}$ for this ion pair. The smallest value of τ_{kc} in DMSO is due to the strongly negative oscillations of $\xi_N(t)$ observed until 0.5 ps, while only mildly negative oscillations of $\xi_N(t)$ were observed for shorter periods in water[33] (up to 0.1 ps) and in methanol[35] (up to 0.2 ps). As in the case of the Na^+-Cl^- ion pair, the trend in the kernel correlation times is attributed to the differences in the behavior of the solvent molecules during the reaction. The liquid structure of methanol is made up of small linear chains of the methanol molecules connected by hydrogen bonding, though the hydrogen bonding in methanol is not as extensive as in water.[16] In the present case, as the ions have the same charges, each of the three solvents will have their oxygen atoms oriented toward the Na^+ ions. The reactant Na^+-Na^+ ion pair resides in the polarization caging regime,[46] because for each of the solvents the ratio $\xi(0)/\omega_b^2$ is much larger than unity in all three solvents. The trend in the kernel correlation time (τ_{kc}) is thus dictated strongly by the extent of hydrogen bonding in the solvents; that is, the strongest hydrogen-bonded solvent should have the longest τ_{kc}. Hence, τ_{kc}(water) > τ_{kc}(methanol) > τ_{kc}(DMSO).

Apart from representing the dynamical role of the solvent, the initial value of the friction kernel, $\xi(0)$, dictates the resultant behavior of the reacting system to be either in the nonadiabatic regime or in the polarization caging regime.[46] For the Na^+-Na^+ ion pair, we observe, $\xi(0)$(methanol) < $\xi(0)$(water) ≪ $\xi(0)$(DMSO). The explanation for the trend is similar to that given for the Na^+-Cl^- ion pair. The large negative values of the square of the nonadiabatic barrier frequencies ω_{NA}^2 and the magnitudes of the ratio $\xi(0)/\omega_b^2$ being much larger than unity for all three solvents indicate strong polarization caging of the Na^+-Na^+ ion pair by the respective solvent molecules. The computed values of Kramers transmission coefficients (κ_{Kr}) follow the trend [κ_{Kr}(DMSO) > κ_{Kr}(methanol) > κ_{Kr}(water)] dictated by the magnitudes of the respective barrier frequencies. The Grote−Hynes transmission coefficients (κ_{GH}) do not follow the trend dictated by the magnitudes of the barrier frequencies, because they depend on the reactive frequency λ_r, which in turn depends on the friction kernel in a more elaborate manner.

5. Reactive Flux Method

The reactive flux technique is commonly used to calculate rate constants by computer simulation.[6−8,13,56,57] For the Na^+-Cl^- ion pair, the pmf can be used to divide the interionic separations into reactants (CIP) and products (SSIP), while the transition state is characterized by an interionic separation ($r = r^{\ddagger} = 4.9$ Å) between the CIP and the SSIP at which the pmf has the highest value. An activation barrier of ca. 28.7 k_BT exists in the pmf of the ion pair in DMSO[30] for the CIP to SSIP conversion. Thus, the passage from the CIP to SSIP configuration involves reactant motion over this activation barrier. For the reverse process, the association barrier is about 1.9 k_BT. That is, for the conversion of SSIP into CIP, the reactant is required to cross this association barrier. An upper cutoff[30] of $r_m = 7.8$ Å is introduced in order to distinguish the SSIP species from the free ions. However this cutoff has no effect on the results of the MD simulations[13] since, for the time scale considered for the simulations (5.0 ps), no ion pairs are observed to dissociate into free ions. Assuming a first-order macroscopic rate law for both the species, one can write[13]

$$dn_c(t)/dt = -k_f n_c(t) + k_r n_s(t) \tag{15a}$$

$$dn_s(t)/dt = k_f n_c(t) - k_r n_s(t) \tag{15b}$$

where n_c and n_s are the average number densities of the CIP and SSIP; k_f and k_r are the forward and reverse rate constants, respectively. These two rate constants are related by the CIP ⇔ SSIP equilibrium constant, $K_{eq} = k_f/k_r$. Usually the forward rate constant k_f is determined from a dynamical simulation, and the reverse rate constant k_r is calculated from the equilibrium constant relation.[13,29] The forward rate constant k_f may be computed from the plateau value in time of the quantity $k_f(t)$ defined by[6]

$$k_f(t) = \frac{\langle (v \cdot \hat{r})\, \delta(r - r^{\ddagger})\, \theta(r(t) - r^{\ddagger}) \rangle}{\langle \theta(r^{\ddagger} - r) \rangle} \tag{16}$$

The angular brackets denote an average over an equilibrium canonical ensemble, v is the relative velocity of the reactant ion pair, and θ is the Heaviside step function. For the present work, v is taken to be positive in the direction of increasing interionic separation. The step function $\theta(x)$ in the numerator ensures that the reaction coordinate is greater than its transition state value, while the delta function $\delta(x)$ localizes the system at the transition state. A special MD method would be needed to evaluate $k_f(t)$, which involves sampling of the equilibrium initial conditions at the transition state.[7] The TST result, k_f^{TST}, for the forward rate constant is the equilibrium one-way flux[58] across the transition state surface ($r = r^{\ddagger}$) in the direction CIP → SSIP.

$$k_f^{TST} = \frac{\langle (v\cdot\hat{r})\,\theta(v\cdot\hat{r})\,\delta(r - r^{\ddagger})\rangle}{\langle \theta(r^{\ddagger} - r)\rangle} \tag{17a}$$

$$= (2\pi\beta\mu)^{-1/2}\,(r^{\ddagger})^2\exp[-\beta W(r^{\ddagger})]/\{\int_0^{r^{\ddagger}} dr\, r^2 \exp[-\beta W(r)]\} \tag{17b}$$

where $\beta = (k_B\,T)^{-1}$, μ is the reduced mass, and $W(r)$ is the pmf of the ion pair. The TST rate assumes that every trajectory at $r^{\ddagger}$ with interionic velocity directed toward the SSIP spatial region is a reactive trajectory.[58] Due to the solvent-induced recrossing at the barrier top, the actual rate deviates from this value. The transmission coefficient is the measure of this departure.

$$\kappa = k_f/k_f^{TST} \tag{18}$$

The transmission coefficient κ is determined in the MD simulation by the plateau value in time of the time dependent transmission coefficient $\kappa(t)$, defined by

$$\kappa(t) = \frac{k_f(t)}{k_f^{TST}} = \frac{\langle (v\cdot\hat{r})\,\theta(v\cdot\hat{r})\,\delta(r - r^{\ddagger})\,[\theta(r(t) - r^{\ddagger}_{-}) - \theta(r(-t) - r^{\ddagger}_{+})]\rangle}{\langle (v\cdot\hat{r})\,\theta(v\cdot\hat{r})\,\delta(r - r^{\ddagger})\rangle} \tag{19}$$

Equation 19 uses the time reversal symmetry and $r^{\ddagger}_{\pm} = (r^{\ddagger} \pm \epsilon)$, $\epsilon > 0$. The infinitesimal quantity ϵ ensures $\kappa(t{=}0) = 1$. The estimation of $\kappa(t)$ involves sampling from a canonical set of initial conditions propagated forward and backward in time from the transition state. This approach was used by Ciccotti et al.[13] in their studies of the ion pair interconversion in model polar solvents.

The time dependent transmission coefficient $\kappa(t)$ was calculated using the scheme as proposed by Carter et al.[12] and applied by Ciccotti et al.[13] A long MD simulation ($\sim$1 ns) was carried out with the interionic separation constrained at $r = r^{\ddagger}$ for generating equilibrium DMSO configurations with the reactant ion pair fixed at the transition state. We have used dynamically independent initial solvent configurations, each separated by 5 ps, to estimate the averages in eq 19. The interionic separation was kept fixed at $r = r^{\ddagger}$, and the momentum associated with this coordinate was also zero. At $t = 0$, the constraint was released, Maxwellian velocities were sampled for the reactant ion pair, and the activated trajectory was followed for a time of $\pm$5 ps.

Figure 6 shows the results for the dynamical transmission coefficient $\kappa(t)$ as a function of time for the Na^+-Cl^- ion pair in DMSO. We find that a well-defined plateau value is established after about 0.4 ps, and the estimated transmission coefficient is 0.11 ± 0.05. After a plateau value is reached for $\kappa(t)$, a macroscopic rate law description holds good for the CIP $\leftrightarrow$ SSIP interconversion. The quite small magnitude of κ_{MD} obtained through direct MD simulation is in fair agreement with the values of κ_{Kr} and κ_{GH} for the Na^+-Cl^- ion pair, as seen in section 4 of the present work. We have already reported the K_{eq} value of CIP $\leftrightarrow$ SSIP equilibrium in our earlier paper[30] to be 1.5×10^{-8} at 298 K. The computed values of the rate constants are given in Table 6. The k_f^{TST} rate constant was evaluated using eq 17b. The smaller value of k_r^{TST} (2.33×10^{-4} ps^{-1}) for the Na^+-Cl^- ion pair in DMSO as compared with the value of k_r^{TST} (5.2×10^{-2} ps^{-1} for the model polar solvent[13] with dipole moment 2.4 D and 8.6×10^{-3} ps^{-1} for the model polar solvent with dipole moment 3.0 D for the same ion pair) seems to be due to the longer length of the SSIP region in DMSO solvent, which is from 4.9 to 7.8 Å.

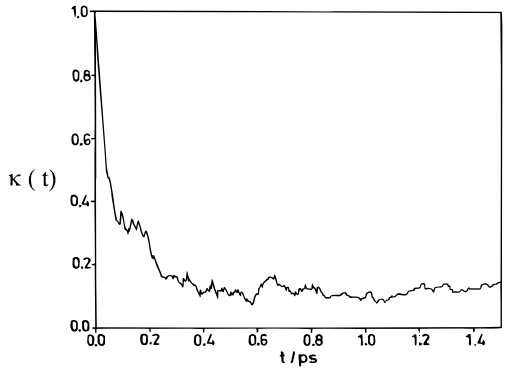

Figure 6. Dynamical transmission coefficient $\kappa(t)$ versus time. κ is estimated from the plateau value of the curve.

TABLE 6: Interconversion Rate Constants and the Transmission Coefficient

k_f^{TST} (s^{-1})	k_f (s^{-1})	k_r^{TST} (ps^{-1})	k_r (ps^{-1})	κ_{MD}
3.50	0.38	2.33×10^{-4}	2.56×10^{-5}	(0.11 ± 0.05)

In Figure 7, we have presented several representative trajectories for the reactant ion pair that give a clear indication of the extensive recrossing in the barrier region.[46] These recrossings are responsible for the marked deviations from the TST and, consequently, the small magnitude of the transmission coefficient. For the Na^+-Cl^- ion pair, we have found that there are approximately three DMSO molecules tightly bound to the CIP configuration, four to five DMSO molecules associated with the transition state, and five DMSO molecules bound to the SSIP configuration. Figure 2 shows detailed pictures of representative solvent configurations at these interionic distances. In all three situations, the sodium end of the reactant ion pair forms a solvation shell, with oxygen atoms of DMSO staying closer to the ion within a radius of 2.1−2.5 Å. At the chloride end, both sulfur and methyl groups compete to form the solvation shell, with the radial distribution functions of (Cl^-−S) and (Cl^-−CH_3) showing the first peak positions at 4.8 and 3.7 Å, respectively. In accordance with the Hammond postulate,[13,59] the transition state solvent configuration resembles more closely that of the SSIP solvent configuration for the Na^+-Cl^- ion pair in DMSO. As the ions separate, the coordination shells around the ions formed by the atoms of the solvent also change. This was analyzed by calculating the running coordination numbers for the ions[16] at the three configurations, namely, the CIP, the transition state, and the SSIP. Table 7 presents the pair distances and coordination numbers for the Na^+-O and the Cl^-−CH_3 pairs. We observe that the ion−solvent coordination shells grow around each ion as the interionic distance is increased. In the Na^+-O case, the running coordination numbers are calculated by integrating the corresponding $g(r)$ up to the first minimum in this $g(r)$, which occurs at 3.8 Å. We see that for the Na^+-O pair, the coordination number increases from 3.2 (CIP) to 4.6 (transition state) and finally to 5.1 (SSIP). In the case of the Cl^-−CH_3 pair, the $g(r)$ has been integrated up to 5.0 Å. This distance is the location of the minimum in the Cl^-−CH_3 radial distribution function when the Na^+-Cl^- ion pair separation is at 2.6 Å. Although the location of this minimum shifts to larger distances (up to 5.9 Å) at the SSIP, we have integrated up to 5.0 Å to show the relative growth in the solvation structure around the chloride ion up to this separation. It is seen from the table that the coordination numbers for the Cl^-−CH_3 pair grow from 9.0 (CIP) to 10.5 (transition state) and finally to 11.0 (SSIP). The

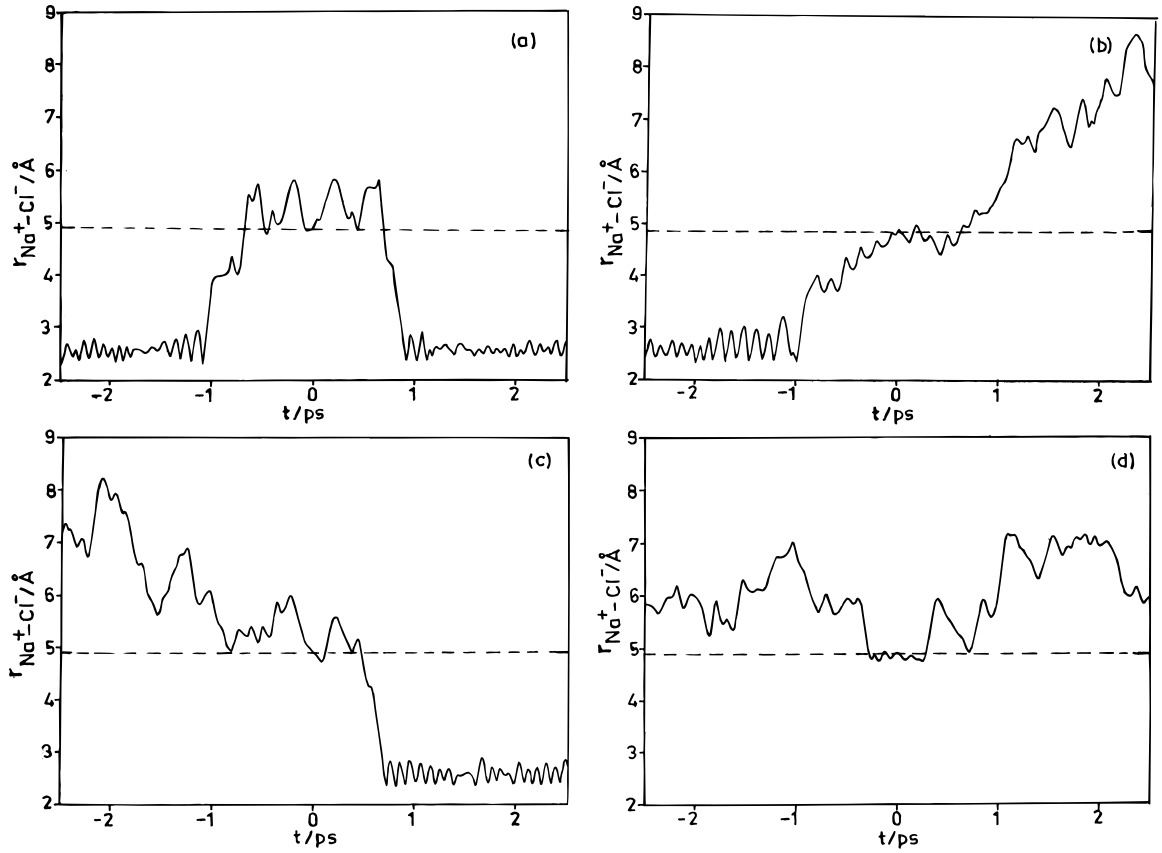

Figure 7. Representative trajectories illustrating the multiple recrossing character of the ion pair dynamics in the barrier region. The transition state surface ($r = r^{\ddagger}$) is also indicated: (a) CIP → CIP (b) CIP → SSIP (c) SSIP → CIP (d) SSIP → SSIP.

TABLE 7: Pair Distances and Coordination Numbers (CN) for the Na^+ and Cl^- Ions in DMSO

	$r(Na^+-Cl^-) =$ 2.6 Å		$r(Na^+-Cl^-) =$ 4.9 Å		$r(Na^+-Cl^-) =$ 7.2 Å	
pair	distance (Å)	CN[a]	distance (Å)	CN[a]	distance (Å)	CN[a]
Na^+-O	2.1	3.2 (3.8)	2.1	4.6 (3.8)	2.1	5.1 (3.8)
Cl^--CH_3	3.7	9.0 (5.0)	3.7	10.5 (5.0)	3.7	11.0 (5.0)[a]

[a] Obtained by the integration of the first peaks of the different radial distribution functions. The values in parentheses next to the coordination numbers are the cutoff distances (in Å) used in the integration.

growth of the structures around the ion pairs has already been shown in detail in Figure 2. These results clearly indicate the larger structural rearrangement around the sodium ion as one goes from the CIP to the SSIP configuration leading to a more strongly solvated cation as the SSIP separates into fully dissociated ions.

We have computed an ensemble of 200 trajectories that start from the pmf barrier top at $r = r^{\ddagger} = 4.9$ Å. These were classified into four types depending on the reactant and product states [namely, CIP → CIP (type I), CIP → SSIP (type II), SSIP → CIP (type III), and SSIP → SSIP (type IV)], which were determined respectively from the backward and forward time evolution from the transition state. Roughly, we have considered the ion pair to be in the CIP well if the interionic distance is less than 3.5 Å and to be in the SSIP well if the distance is more than 6.5 Å. We found that about 20% of the trajectories represent type I, 12% represent type II, 8% represent type III, and the rest represent type IV. The representative trajectories in Figure 7 exemplify each of these types. It is clearly seen that when an activated trajectory travels from the CIP to the SSIP region or vice versa in the configuration space, multiple recrossings occur. In Figure 7b, we see that there are six recrossings (per ps) for the CIP → SSIP, and in Figure 7c, we have four recrossings (per ps) for the SSIP → CIP conversion. Also, the fate of an activated trajectory originating at the transition state ($r = r^{\ddagger}$) is decided within a time interval of less than 0.5 ps. The recrossing dynamics induced by the presence of the solvent brings down the value of the rate constant much below the TST predicted value.

6. Conclusions

Constrained MD simulations have been performed to study several dynamical aspects of the CIP ⇔ SSIP process for a sodium chloride ion pair in dimethyl sulfoxide. We have calculated the solvent friction kernels for Na^+-Cl^-, Na^+-Na^+, and Cl^--Cl^- ion pairs in DMSO. The friction kernels in DMSO show many similarities to the friction kernels in water and in methanol. Each of these have a very rapid short-time decay, followed by an oscillatory long-time decay. As the DMSO solvent molecules are fairly large, they tend to solvate the reactant ion pair jointly even at large interionic separations of ~7 Å. This makes the SSIP configuration a less preferred one, even at large interionic separations, a fact supported by the very deep potential minimum in the ion−ion potential of mean force. Earlier calculations of the solvent friction kernels for the three ion pairs in water and in methanol emphasized the dependence of the initial value $\xi(0)$ of the friction kernel on interionic separation. In the present study, the initial values of the friction kernels for the Na^+-Cl^- ion pair in DMSO do not show the proportionate increase with increasing interionic separation, as observed in the case of water and methanol. In contrast, the Na^+-Na^+ ion pair in DMSO shows increased value of the friction kernel with increasing interionic distance. This was also observed in methanol, but not in the case of water. For the Cl^--Cl^- ion pair, the $\xi(0)$ values in DMSO remain

more or less unchanged with increasing interionic distance, while the same in water showed an increase.

As regards the very small magnitude of the transmission coefficient, calculated either by the Kramers theory or by the Grote−Hynes theory, we are led to believe that the TST is not generally applicable to these activated processes in solution.[11,13,28,29,35] In the Kramers formula, the constant friction coefficient ξ (eq 9) of the time dependent friction kernel $\xi(t)$ is used to account for the solvent frictional forces. This is not strictly correct, as the dynamical $\kappa(t)$ reaches a plateau value only after ~0.4 ps (Figure 6). The long-time tail of $\xi(t)$ (which extends for $t \gg 0.4$ ps) contributes significantly to the constant friction coefficient (eq 10). The Grote−Hynes theory[38,46] expresses the transmission coefficient in terms of the full time dependent friction kernel, $\xi(t)$, of the solvent associated with the reactive motion of the ion pair at the barrier top. In conjunction with the direct MD $\kappa(t)$, it is thus evident that the shorter time components of $\xi(t)$ are the most important[13] (i.e. less than 0.4 ps). Due to extensive solvent-induced recrossings of the top of the barrier in the pmf, the computed value of κ_{MD} is considerably less than the TST prediction.

We have analyzed the ion pair interconversion processes involving Na^+-Cl^- and Na^+-Na^+ pairs in DMSO. However, since the pmf of the Cl^--Cl^- ion pair does not possess any local maximum or minimum in DMSO, such an analysis could not be performed in this case. For the description of the nonequilibrium solvation and the participation of the solvent in chemical reactions in solution, the quantity of interest is the square of the nonadiabatic barrier frequency, ω_{NA}^2. We have calculated ω_{NA}^2 for both Na^+-Cl^- and Na^+-Na^+ barrier crossing reactions in DMSO. The large negative magnitude of this quantity ($\omega_{NA}^2 = -9.9 \times 10^3$ ps^{-2} for Na^+-Cl^- and $\omega_{NA}^2 = -7.9 \times 10^3$ ps^{-2} for Na^+-Na^+) advocates the fact that the solvent instantaneously traps the reactant ion pair in a polarization cage, around which the relative motion of the solvent molecules dictates the stability of the CIP/SSIP. This is in agreement with the prediction of a very stable CIP configuration (depth of the potential well equals 28.7 k_BT) for the Na^+-Cl^- ion pair.

As an extreme limit of the polarization caging regime, when $\tau_{kc} \ll \lambda_r^{-1}$ (τ_{kc} is the kernel correlation time and λ_r^{-1} is the reaction time), the reactant system resides in the adiabatic regime. Under such circumstances, the predictions of the Grote−Hynes theory reduce to those of the Kramers theory, making the values of κ_{GH} and κ_{Kr} nearly identical. In DMSO, observed values for τ_{kc} and λ_r^{-1} are 0.025 and 1.56 ps, respectively, for Na^+-Cl^-, while for Na^+-Na^+, the same are 0.02 and 0.83 ps, respectively. Our observations confirm that for Na^+-Cl^-, $\kappa_{GH} = \kappa_{Kr} = 0.05$, while for Na^+-Na^+, κ_{GH} is 0.08 and κ_{Kr} is 0.09. We would like to note that if we use $t_{0.05}$ in place of τ_{kc} and compare this with λ_r^{-1}, we find that $t_{0.05} < \lambda_r^{-1}$ for both the ion pairs in DMSO and that $\kappa_{GH} = \kappa_{Kr}$. Extending this analogy to the other two solvents, viz., water and methanol, we find that for the Na^+-Cl^- ion pair in water τ_{kc} is 0.10 ps while λ_r^{-1} is 0.28 ps and that κ_{GH} (0.22) $\neq \kappa_{Kr}$ (0.18). In this case, $t_{0.05}$ (0.79 ps) > λ_r^{-1} and the system is not in the adiabatic regime. A similar conclusion also holds for the Na^+-Cl^- ion pair in methanol. For the Na^+-Na^+ ion pair in water the system is once again in the adiabatic regime as τ_{kc} (0.13 ps) $\ll \lambda_r^{-1}$ (4.50 ps). In this case, $t_{0.05}$ (0.78 ps) is again smaller than λ_r^{-1}. Finally, the Na^+-Na^+ ion pair in methanol deviates slightly from the adiabatic regime as τ_{kc} (0.08 ps) is not really much smaller than λ_r^{-1} (0.56 ps) and κ_{GH} (0.12) $\neq \kappa_{Kr}$ (0.07). We note that in this case also $t_{0.05}$, which is 0.44 ps, is comparable to the reaction time scale λ_r^{-1}. Thus we find that the value of $t_{0.05}$ can also be used for comparison with the reaction time scales.

Detailed features of the reaction mechanism depend strongly on the reorganization of the solvent molecules around the reactant ion pair. For the Na^+-Cl^- pair, four DMSO molecules are found to be tightly bound to the CIP, six to seven molecules are seen to be associated with the transition state, and eight DMSO molecules surround the ion pair to form the SSIP (Figure 2). In all these configurations, oxygen atoms form the coordination shell at the Na^+ end; sulfur atoms compete with the methyl groups to form the coordination shell at the Cl^- end. The distance dependence of the growth of the solvation shell around the reactant ion pair has been monitored by calculating the running coordination numbers. For the (Na^+-O) shell, the coordination number (when the integration of $g(r)$ is performed up to 3.8 Å) changes from 3 (CIP) to 4−5 (transition state) to 5 (SSIP). For the (Cl^--CH_3) shell, the coordination number (when the integration of $g(r)$ is performed up to 5.0 Å) changes from 9 (CIP) to 10−11 (transition state) to 11 (SSIP). From these data, it is evident that the closest coordination shells of the respective ions change significantly when the ion pair moves from a CIP to the transition state and finally to the SSIP. As the solvent coordination gets changed during the passage of CIP to SSIP and vice versa, one concludes that the interconversion process involves considerable solvent reorganization, especially toward the strongly bound sodium end.

Acknowledgment. We would like to thank the Department of Science and Technology, Government of India, and the Indian Institute of Technology, Bombay, for the computational support provided for this work. We are extremely grateful to the reviewers for their constructive criticism, which encouraged us to verify the values of the theoretical rate constants by direct MD simulations.

References and Notes

(1) Burgess, J. *Ions in Solution: Basic Principles of Chemical Interactions*; Ellis Horwood Limited: Chichester, U.K., 1988.
(2) Smid, J., Ed. *Ions and Ion Pairs and their Role in Chemical Reactions*; Pergamon Press: Oxford, U.K., 1979.
(3) Connors, K. A. *Chemical Kinetics: The Study of Reaction Rates in Solution*; VCH Publishers Inc.: New York, 1990.
(4) Funel, M. C. B., Neilson, G. W., Eds. *The Physics and Chemistry of Aqueous Ionic Solutions*; D. Reidel Publishing Co.: Dordrecht, Holland, 1987.
(5) Hynes, J. T. In *Theory of Chemical Reaction Dynamics*; Baer, M., Ed.; CRC Press: Boca Raton, FL, 1985.
(6) Yamamoto, T. *J. Chem. Phys.* **1960**, *33*, 281.
(7) Chandler, D. *Introduction to Modern Statistical Mechanics*; Oxford University Press: New York, 1987.
(8) Brooks, C. L.; Karplus, M.; Pettitt, B. M. *Adv. Chem. Phys.* **1988**, *71*, 1.
(9) Ciccotti, G., Frenkel, D., McDonald, I. R., Eds. *Simulation of Liquids and Solids: Molecular Dynamics and Monte Carlo Methods in Statistical Mechanics*; North-Holland Physics Publishing: Amsterdam, 1987.
(10) Karim, O. A.; McCammon, J. A. *J. Am. Chem. Soc.* **1986**, *108*, 1726.
(11) Karim, O. A.; McCammon, J. A. *Chem. Phys. Lett.* **1986**, *132*, 219.
(12) Carter, E. A.; Ciccotti, G.; Hynes, J. T.; Karpal, R. *Chem. Phys. Lett.* **1989**, *156*, 472.
(13) Ciccotti, G.; Ferrario, M.; Hynes, J. T.; Kapral, R. *J. Chem. Phys.* **1990**, *93*, 7137.
(14) Jacob, S. W.; Rosenbaum, E. E.; Wood, D. C. *Dimethyl Sulphoxide: Basic Concepts of DMSO*; Marcel Dekker, Inc.: New York, 1971.
(15) Krapcho, A. P. *Synthesis* **1982**, 805; *Synthesis* **1982**, 893.
(16) Rao, B. G.; Singh, U. C. *J. Am. Chem. Soc.* **1990**, *112*, 3803.
(17) Vaisman, I. I.; Berkowitz, M. L. *J. Am. Chem. Soc.* **1992**, *114*, 7889.
(18) Luzar, A.; Chandler, D. *J. Chem. Phys.* **1993**, *98*, 8160.
(19) Petitt, B. M.; Rossky, P. J. *J. Chem. Phys.* **1986**, *84*, 5836.
(20) Levesque, D.; Weiss, J. J.; Patey, G. N. *Mol. Phys.* **1979**, *38*, 1635.
(21) Patey, G. N.; Carnie, S. L. *J. Chem. Phys.* **1983**, *78*, 5183.
(22) Morita, T.; Ladanyi, B. M.; Hynes, J. T. *J. Phys. Chem.* **1989**, *93*, 1386.

(23) Kusalik, P. G.; Patey, G. N. *J. Chem. Phys.* **1990**, *92*, 1345.
(24) Berkowitz, M.; Karim, O. A.; McCammon, J. A.; Rossky, P. J. *Chem. Phys. Lett.* **1984**, *105*, 577.
(25) Belch, A.; Berkowitz, M.; McCammon, J. A. *J. Am. Chem. Soc.* **1986**, *108*, 1755.
(26) Jorgensen, W. L.; Buckner, J. K.; Houston, S. E.; Rossky, P. J. *J. Am. Chem. Soc.* **1987**, *109*, 1981.
(27) Dang, L. X.; Petitt, B. M. *J. Chem. Phys.* **1987**, *86*, 6560.
(28) Ciccotti, G.; Ferrario, M.; Hynes, J. T.; Kapral, R. *Chem. Phys.* **1989**, *129*, 241.
(29) Rey, R.; Guardia, E. *J. Phys. Chem.* **1992**, *96*, 4712.
(30) Madhusoodanan, M.; Tembe, B. L. *J. Phys. Chem.* **1995**, *99*, 44.
(31) McQuarrie, D. A. *Statistical Mechanics*; Harper and Row; New York, 1976.
(32) Wolynes, P. G. *J. Chem. Phys.* **1978**, *68*, 473.
(33) Rey, R.; Guardia, E.; Padro, J. A. *J. Chem. Phys.* **1992**, *97*, 1343.
(34) Guardia, E.; Rey, R.; Padro, J. A. *J. Chem. Phys.* **1991**, *95*, 2823.
(35) Sese, G.; Guardia, E.; Padro, J. A. *J. Phys. Chem.* **1995**, *99*, 12647.
(36) Madhusoodanan, M.; Tembe, B. L. *J. Phys. Chem.* **1994**, *98*, 7090.
(37) Kramers, H. A. *Physica* **1940**, *7*, 284.
(38) Grote, R. F.; Hynes, J. T. *J. Chem. Phys.* **1980**, *73*, 2715.
(39) Bertagnolli, H.; Schultz, E.; Chieux, P. *Ber. Bunsen-Ges Phys. Chem.* **1989**, *93*, 88.
(40) Allen, M. P.; Tildesley, D. J. *Computer Simulation of Liquids*; Clarendon Press: Oxford, 1987.
(41) Hansen, J. P.; McDonald, I. R. *Theory of Simple Liquids*; Academic Press: San Diego, 1990.
(42) Verlet, L. *Phys. Rev.* **1967**, *159*, 98.
(43) Ryckaert, J. P.; Ciccotti, G.; Berendsen, H. J. C. *J. Comput. Phys.* **1977**, *23*, 327.
(44) Berne, B. J.; Tuckerman, M. E.; Straub, J. E.; Bug, A. L. R. *J. Chem. Phys.* **1990**, *93*, 5084.
(45) Guardia, E.; Rey, R.; Padro, J. A. *Chem. Phys.* **1991**, *155*, 187.
(46) van der Zwan, G.; Hynes, J. T. *J. Chem. Phys.* **1982**, *76*, 2993.
(47) Grote, R. F.; van der Zwan, G.; Hynes, J. T. *J. Phys. Chem.* **1984**, *88*, 4676.
(48) van der Zwan, G.; Hynes, J. T. *Chem. Phys.* **1984**, *90*, 21.
(49) (a) Zichi, D. A.; Hynes, J. T. *J. Chem. Phys.* **1988**, *88*, 2513. (b) Lee, S.; Hynes, J. T. *J. Chem. Phys.* **1988**, *88*, 6863.
(50) (a) Simon, J. D. *Acc. Chem. Res.* **1988**, *21*, 128. (b) Zichi, D. A.; Ciccotti, G.; Hynes, J. T.; Ferrario, M. *J. Phys. Chem.* **1989**, *93*, 6261. (c) Barbara, P. F.; Jarzeba, W. *Adv. Photochem.* **1990**, *15*, 1.
(51) Borgis, D.; Lee, S.; Hynes, J. T. *Chem. Phys. Lett.* **1989**, *162*, 19.
(52) Carter, E. A.; Hynes, J. T. *J. Chem. Phys.* **1991**, *94*, 5961.
(53) (a) Gertner, B. J.; Wilson, K. R.; Hynes, J. T. *J. Chem. Phys.* **1989**, *90*, 3537. (b) Gertner, B. J.; Whitnell, R. M.; Wilson, K. R.; Hynes, J. T. *J. Am. Chem. Soc.* **1991**, *113*, 74.
(54) van der Zwan, G.; Hynes, J. T. *J. Chem. Phys.* **1983**, *78*, 4174.
(55) Hynes, J. T. *J. Phys. Chem.* **1986**, *90*, 3701.
(56) Berne, B. J. In *Multiple Time Scales*; Brackbill, J. U., Cohen, B. I., Eds.; Academic Press: New York, 1985.
(57) Chandler, D.; Kuharski, R. A. *Faraday Discuss. Chem. Soc.* **1988**, *85*, 329.
(58) Pechukas, P. In *Dynamics of Molecular Collisions*, Part B; Miller, W. H.; Ed.; Plenum Press: New York, 1976.
(59) Hammond, G. S. *J. Am. Chem. Soc.* **1955**, *77*, 334.